Aalborg Universitet

Stand-Alone Operation of Distributed Generation Systems With Improved Harmonic Elimination Scheme

Khan, Mohammed Ali; Haque, Ahteshamul; Kurukuru, Varaha Satya Bharath; Wang, Huai; Blaabjerg, Frede

Published in:
I E E E Journal of Emerging and Selected Topics in Power Electronics

DOI (link to publication from Publisher):
10.1109/JESTPE.2021.3084737

Publication date:
2021

Document Version
Accepted author manuscript, peer reviewed version

Link to publication from Aalborg University

Citation for published version (APA):
Khan, M. A., Haque, A., Kurukuru, V. S. B., Wang, H., & Blaabjerg, F. (2021). Stand-Alone Operation of Distributed Generation Systems With Improved Harmonic Elimination Scheme. *I E E E Journal of Emerging and Selected Topics in Power Electronics*, *9*(6), 6924 - 6934. Article 9443217. https://doi.org/10.1109/JESTPE.2021.3084737

General rights
Copyright and moral rights for the publications made accessible in the public portal are retained by the authors and/or other copyright owners and it is a condition of accessing publications that users recognise and abide by the legal requirements associated with these rights.

- Users may download and print one copy of any publication from the public portal for the purpose of private study or research.
- You may not further distribute the material or use it for any profit-making activity or commercial gain
- You may freely distribute the URL identifying the publication in the public portal -

Take down policy
If you believe that this document breaches copyright please contact us at vbn@aub.aau.dk providing details, and we will remove access to the work immediately and investigate your claim.

Downloaded from vbn.aau.dk on: December 04, 2025

This article has been accepted for publication in a future issue of this journal, but has not been fully edited. Content may change prior to final publication. Citation information: DOI 10.1109/JESTPE.2021.3084737, IEEE Journal of Emerging and Selected Topics in Power Electronics

Standalone operation of Distributed Generation Systems with Improved Harmonic Elimination Scheme

Mohammed Ali Khan, *Student Member, IEEE,* Ahteshamul Haque, *Senior Member, IEEE,* V S Bharath Kurukuru, *Student Member, IEEE,* Huai Wang, *Senior Member, IEEE* and Frede Blaabjerg, *Fellow, IEEE*

Abstract- **Improvement in the efficiency of distribution generation (DG) inverters is a concern and challenge for researchers across the globe. To address the concern an inverter control technique is developed. Inverters have issues with voltage regulation and harmonics when operating in the grid-connected (GC) and stand-alone (SA) mode. This paper proposes a control strategy capable of operating DGs in both SA and GC environments. The GC operation of the inverter is achieved by the current control mode and the SA control features a voltage control loop capable of overcoming the drawbacks due to load shedding or load switching. Besides, the harmonics due to various conditions of transition and load switching are eliminated by adapting a harmonic elimination pulse width modulation (PWM) scheme. To enhance the performance of the inverter and eliminate the problem of flexibility associated with conventional and offline switching angle calculations in the PWM technique, a Bio-Inspired Intelligent algorithm is adapted. The developed system is verified for various reduced total harmonic distortions (THD) by performing simulations and experiments. The results depict that the output voltage is regulated for varying load conditions, and the THD is observed to be 2.4% under varying load conditions.**

Keywords - Distributed Generation (DG), Stand-alone (SA) mode, Selective harmonic elimination, Pulse width modulation, Voltage regulation, Total harmonic distortion.

I. INTRODUCTION

The advancements in distributed generation systems (DGs) and the decreasing investment costs have encouraged grid integration of DGs. For efficient operation of these systems with the existing power systems, power electronics-based converters are utilized [1]. In general, most of the DGs generate DC power or convert generated power to DC, and then convert it to AC using a full-bridge inverter. This full-bridge inverter achieves integration between the DC bus and the utility through a controller, to provide the benefits as improved power quality, voltage support, diversification of power sources, and enhancing the utility.

Apart from the advantages, the integration of DGs needs to address some issues and concerns regarding the design and support of power delivery during grid-connected (GC) and stand-alone (SA) modes of operation. While operating in a GC mode, the DG injects pre-set power to the grid through a current control mode in a stiff synchronization with the grid [2], [3]. When the DG system is disconnected from the grid due to unplanned faulty events or for planned maintenance, it needs to operate with the local loads in a voltage control mode (SA operation) [4], [5]. In this mode, DG should address the issues of voltage and frequency regulation and maintain a balance between load and supply.

Conventionally, while operating in SA mode, the usage of carrier-based pulse width modulation (PWM) [6], [7], space vector PWM [8], and repetitive control techniques [9] has offered accurate but slow voltage regulation and harmonic compensation in the system. Apart from these, a wide literature is available [10], [11] regarding the voltage regulation in SA systems. Many researchers have been working with a dual-loop control strategy being implemented in the hybrid frame of reference [12]. It aims at better efficiency and optimum performance of the system under the delay caused by the controller. Further, a forced switching sliding mode control was presented in [13] to achieve efficient control of dual inverters in SA operation of single-stage PV systems. The control scheme maintains the desired voltage at the DC link capacitor using a PI-based vector control along with the forced switch-based vector control. In [14], [15], the model predictive control is used as a voltage control strategy for a single-phase inverter operating in SA mode. The developed controller predicts the output voltage of the system on each sampling interval for each possible switching state. Then a cost function is utilized for selecting and applying an appropriate switching state during the next sampling interval.

From the above study, it is observed that the conventional control methods fail to optimally suppress selective harmonics, and the response for voltage regulation during load changes is very slow. To overcome this a voltage regulation technique through current compensation along with selective harmonic elimination (SHE) PWM technique [16] is proposed. The proposed controller adapts voltage compensators for generating the current references in the SA operation of DGs. Further, SHE overcomes the losses due to the absence of fast switching devices. There is a trade-off between switching speed and power handling. With this method, it is possible to eliminate several harmonics, which are directly proportional to the frequency modulation ratio. In the conventional SHE, the sequence of switching angles that define a PWM waveform is calculated by solving a set of transcendental equations [17]. This generally depends on the number of harmonics to be eliminated, which is related to the ratio of the switching frequency to the output frequency of the inverter. The desired amplitude of the fundamental component of the output waveform appears as a parameter in the set of equations. Consequently, the set of equations must

Mohammed Ali Khan, Ahteshamul Haque and V.S. Bharath Kurukuru are with Advance Power Electronics Research Laboratory, Department of Electrical Engineering, Jamia Millia Islamia (A Central University), New Delhi 110025, India
Huai Wang and Frede Blaabjerg are with the Department of Energy Technology, Aalborg University, Aalborg Øst 9220, Denmark.

2168-6777 (c) 2021 IEEE. Personal use is permitted, but republication/redistribution requires IEEE permission. See http://www.ieee.org/publications_standards/publications/rights/index.html for more information.
Authorized licensed use limited to: Aalborg Universitetsbibliotek. Downloaded on June 03,2021 at 09:09:39 UTC from IEEE Xplore. Restrictions apply.

This article has been accepted for publication in a future issue of this journal, but has not been fully edited. Content may change prior to final publication. Citation information: DOI 10.1109/JESTPE.2021.3084737, IEEE Journal of Emerging and Selected Topics in Power Electronics

be solved for each desired amplitude. In [18], the Fourier series analysis based SHE is implemented for undesired harmonic minimization in multi-level inverters. Besides, the Newton Raphson approach is adapted to estimate the possible solutions for transcendental, and highly nonlinear equations in the modulation range. The results showed dynamic solutions for different modulation indices and achieved elimination of lower order odd harmonics from the output voltage. Similarly, the SHE-PWM along with an advanced derivative free numerical technique is used in [19] to achieve optimum switching for multi-level inverter and reduces THD in the output voltage. Further, in [20], a Jacobian estimate based SHE-PWM approach is developed to overcome the drawbacks of singularity for complex calculations of SHE. The developed approach achieved the elimination of non-triplen lower order odd harmonics for the output voltage of multilevel converters. In [21], the particle swarm optimization based SHE-PWM is developed for estimating the switching angles of the power converter operation. The BAT-SHE discussed in [22] suggested by the reviewer mainly focussed on problems while determining optimal switching angles for SHE while eliminating undesired harmonics with multilevel inverter. From the literature it is identified that, the use of Fourier transforms-based Look-Up Tables for solving the arbitrary changes in output voltage amplitudes resulted in slow dynamic responses for the system operation.

Considering the problems with voltage regulation, and harmonics, this paper develops an optimized controller to improve the performance of the system. The major contribution of the developed inverter control scheme is:

- The proposed approach is capable of operating the distributed generation systems (DGs) in both standalone (SA) and grid-connected (GC) environments with less voltage harmonics and without any requirement for additional compensating devices.
- The Bat-selective harmonic elimination (SHE)-pulse width modulation (PWM) scheme eliminates the harmonics due to various conditions of transition and load switching.
- The controller when operated in SA mode with a single-phase inverter regulates the load voltage within the limits for both linear and non-linear loads.

Besides, the tolerance of the controller towards voltage transients and the harmonic rejection capability are some of the major advantages of the proposed controller over the conventional methods. Further sections of the paper are organized as follows: Section II identifies the problems associated with load shedding or switching while operating in SA mode; Section III discusses the development of voltage control loop for standalone operation of DG. Section IV explains the harmonic elimination scheme and its optimization. The simulation and experimental analysis are discussed in Section V and the discussion is concluded in Section VI.

II. Control Method and Load Shedding

The transition between GC and SA modes can be achieved by an over/under voltage method [23] or through over/under frequency methods [24], [25]. Generally, during the GC mode of operation, DG operates in grid feeding/supporting mode according to factors such as energy availability, energy cost, and others [26]. During this process, the grid supplies or absorbs the power difference between the local load and the DG. When a power outage occurs at the grid side, the DG that operated in grid feeding/supporting mode can cause frequency and voltage transients depending on the amount of power difference. Further, the power difference creates a drift between measured and nominal values of voltage and frequency [27]. When the drift value reaches the threshold, the SA controller must be capable of mitigating the transients and perform load shedding to maintain a balance between the supply and demand. This method is applicable for islanding detection and intentional islanding operation. But during unintentional islanding operation, the DG power generation can either be greater than or less than the local load and the controller may find it difficult to overcome the transients during GC to SA operation. Hence, to overcome these drawbacks, an intelligent controller capable of performing load shedding and balancing the voltage and frequency to operate within the limits is required [28]. This provides a challenge of switching the full bridge inverter connected with the DG system to operate in a voltage control mode. The voltage control mode relates to the rate of change of voltage with respect to the power differences between the load demand and DG generation. This helps in regulating the voltage within the limits ($0.88 - 1.1\ V_{pu}$) while operating for load shedding or load switching under SA mode of operation. In order to accomplish this, the system shown in Fig. 1(a) has been analysed as follows:

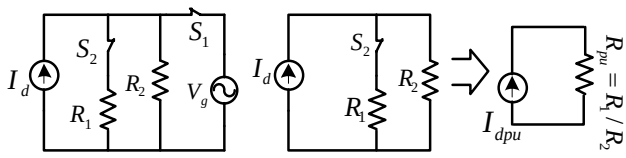

(a) (b)

Fig. 1 Load shedding approach (a) System to implement load shedding, (b) System in per unit to implement load shedding

The required load shedding can be determined using the algorithm based on Fig. 1(b) given as

Algorithm: *Load Shedding Algorithm*

Step 1: Obtain the expression of voltage amplitude (V_{pk}) for load shedding:

From Fig. 1(b), the expression for load voltage V_{pu} is given by:

$$V_{pu} = I_{dpu} R_{pu} \sin(\omega t) \quad (1)$$

where I_{dpu} is the current source in pu, and R_{pu} is the total local load in pu

Using V_{pu}, the voltage amplitude is calculated as:

$$V_{pk} = \sqrt{2} I_{dpu} R_{pu} \sin(\omega t) \quad (2)$$

Step 2: Obtain the slope $\mathcal{S}$ of the voltage amplitude:

$$\mathcal{S} = \frac{d[V_{pk}(t)]}{dt} = \sqrt{2}\omega I_{dpu} R_{pu} \cos(\omega t) \quad (3)$$

Step 3: Obtain the expression for the current source I_{dpu}:

$$I_{dpu} = \frac{\mathcal{S}\sqrt{2}}{2\omega R_{pu} \cos(\omega t)} \quad (4)$$

2168-6777 (c) 2021 IEEE. Personal use is permitted, but republication/redistribution requires IEEE permission. See http://www.ieee.org/publications_standards/publications/rights/index.html for more information.
Authorized licensed use limited to: Aalborg Universitetsbibliotek. Downloaded on June 03,2021 at 09:09:39 UTC from IEEE Xplore. Restrictions apply.

This article has been accepted for publication in a future issue of this journal, but has not been fully edited. Content may change prior to final publication. Citation information: DOI 10.1109/JESTPE.2021.3084737, IEEE Journal of Emerging and Selected Topics in Power Electronics

As $R_{pu} = R_{1pu}//R_{2pu}$, and solving R_{1pu} which represents the load to be shed,

$$R_{1pu} = \frac{\sqrt{2}\omega R_{pu}\cos(\omega t)}{s} \quad (5)$$

III. CONTROL STRATEGY

The proposed voltage loop controller for SA mode operation of an inverter with a seamless transition is provided in Fig. 2. The controller regulates the voltage through current compensation and uses the voltage compensators to generate the current references for current regulation.

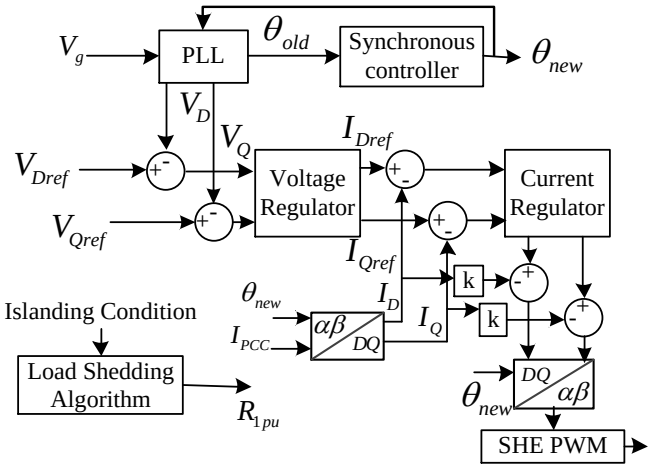

Fig. 2. Voltage control loop for full-bridge inverter operation

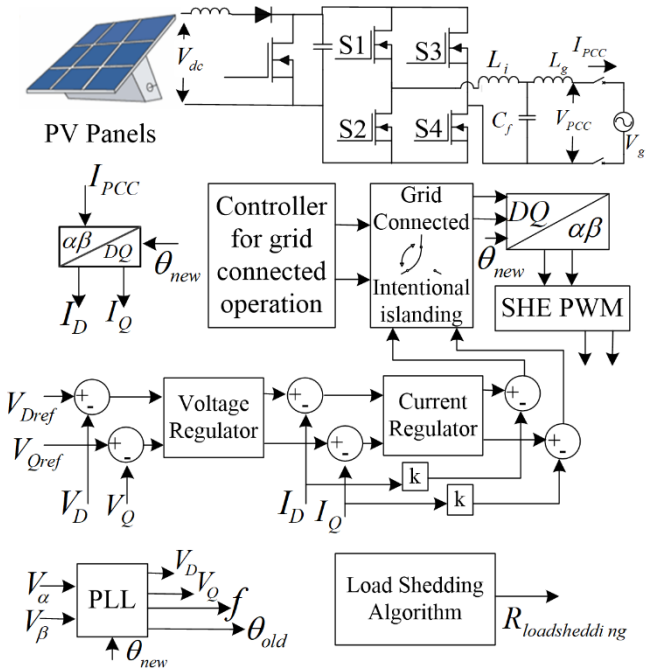

Fig. 3. Schematic of proposed controller action between grid-connected and islanded distributed generation system

From Fig. 2, it can be identified that the direct and quadrature components of the load voltage V_D and V_Q are required to track their reference components V_{Dref} and V_{Qref} respectively using a voltage regulator (proportional-integral (PI) compensator). This results in I_{Dref} and I_{Qref} components, which are compared with the direct and quadrature components (I_D and I_Q) of load current. The difference is fed to a current regulator (PI compensator), which outputs the voltage reference signal fed to the PWM technique. The PWM generates high-frequency gating signals for driving the full-bridge inverter.

The control loop stabilizes the system operation and improves the dynamic responses by compensating the voltage variations during transition and load shedding [29], [30]. Further, an enhanced dynamic response of the controller is achieved by operating the V_{DQ} in feed forward loop, which will compensate for the disturbance due to inverter terminal voltage [31]. Besides, a compensation coefficient K is added along with the current controller to act as a feed-forward controller, which processes the magnitude of the input voltage of the PWM and realizes an accurate tracking of a sinusoidal reference. This provides a counterattack to severe transitions that are influenced by the disconnection of the inverter from the grid. A block representation of the proposed controller action between GC and SA-DGs system is given in Fig. 3.

IV. HARMONIC ELIMINATION TECHNIQUE

In general, the power disturbances which regularly effects the operation of a power system can be divided into two different categories considering the duration of disturbance. They are static problems like under/overvoltage's, total harmonic distortion and transient problems like voltage sags, and momentary disturbance.

Considering the operation of power electronic devices, it can be stated that they produce substantial harmonics in voltage due to their abrupt chopping behaviour. The semiconductor switches chop the voltage waveforms during their transition between conducting and cut-off states. In view of these effects, the inverter circuits are considered as a major source for producing harmonics and are used widely today.

In order to minimize the effect of harmonics and mitigate them selective harmonic elimination PWM switching is adapted. In conventional SHE, the sequence of switching angles that define a PWM waveform is calculated by solving a set of transcendental equations. The size of the set of equations depends on the number of harmonics to be eliminated, which is related to the ratio of the switching frequency to the output frequency of the inverter. The desired amplitude of the fundamental component of the output waveform appears as a parameter in the set of equations. Consequently, the set of equations must be solved for each desired amplitude, but there is no method for solving these equations in real time for an arbitrary amplitude. In order to achieve this, advanced optimizing techniques need to be adapted with SHEPWM to calculate the switching angles.

A. Selective Harmonic Elimination PWM

A generalized method to eliminate any number of harmonics is done by switching the voltage waveform. For a periodic inverter voltage waveform with unit amplitude, this relationship is easily derived without losing generality using the SHE PWM. The SHE technique makes use of Fourier series analysis of the periodic output waveform to establish a set of transcendental equations that can be solved to

2168-6777 (c) 2021 IEEE. Personal use is permitted, but republication/redistribution requires IEEE permission. See http://www.ieee.org/publications_standards/publications/rights/index.html for more information.
Authorized licensed use limited to: Aalborg Universitetsbibliotek. Downloaded on June 03,2021 at 09:09:39 UTC from IEEE Xplore. Restrictions apply.

This article has been accepted for publication in a future issue of this journal, but has not been fully edited. Content may change prior to final publication. Citation information: DOI 10.1109/JESTPE.2021.3084737, IEEE Journal of Emerging and Selected Topics in Power Electronics

determine switching angles that result in selected harmonics having zero amplitude [32]. With this method, it is possible to eliminate several harmonics directly proportional to the frequency modulation ratio. It is only necessary to solve for these angles, because of the symmetry of the waveform.

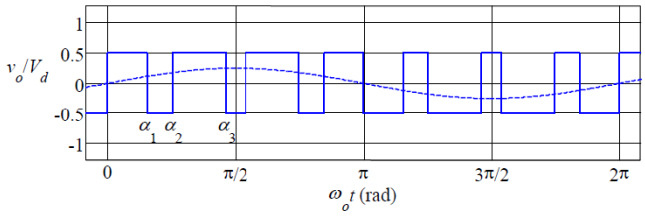

Fig. 4. Quarter-Wave Symmetric PWM Waveform

Fig. 4 shows a generic PWM output where α denotes the desired switching angles for the first quarter of the waveform. For the waveform in Fig. 4, the half-wave symmetry and the Fourier series are given as:

$$f(\omega t) = \sum_{1,2.3}^{\infty}[b_k \sin(k\omega t) + a_k \cos(k\omega t)] \quad (6)$$

The switching angles $\alpha_0 = 0$, $\alpha_{2M+1} = \pi$ where $\alpha_0 < \alpha_1 < \alpha_2 < \cdots < \alpha_{2M+1}$ are used for deriving the values of harmonic coefficients a_k and b_k. From the half-wave symmetry proper, for all odd values of k:

$$a_k = 4/k\pi[-\sum_{n=1}^{2M}(-1)^n \sin(k\alpha_n)], \text{ and} \quad (7)$$

$$b_k = 4/k\pi[1 + \sum_{n=1}^{2M}(-1)^n \cos(k\alpha_n). \quad (8)$$

where k is the order of harmonics that will be considered. These harmonic coefficients correspond to a function of 2M variables. Hence, by equating M harmonics to zero and applying quarter-wave symmetry:

$$\alpha_n = \pi - \alpha_{2M-n+1} \text{ for } n = 1,2,3, M \text{ and } a_k = 0. \quad (9)$$

Thus,

$$b_k = 4/k\pi[1 + \sum_{n=1}^{M}(-1)^n \cos(k\alpha_n). \quad (10)$$

For the sake of simplicity, only three odd harmonics will be considered in this analysis, which defines the harmonic coefficient as:

$$b_k = \frac{4\frac{v_0}{v_d}}{\pi k}[1 - 2\cos(k\alpha_1) + 2\cos(k\alpha_2) - 2\cos(k\alpha_3)] \quad (11)$$

where, v_o is the output voltage, V_d is the desired voltage, and α is the desired switching angle.

For more than 3 switching angles, the equation can be generalized as:

$$b_k = \frac{4\frac{v_0}{v_d}}{\pi k}[1 - 2\cos(k\alpha_1) + 2\cos(k\alpha_2) - 2\cos(k\alpha_3) + \cdots + (-1)^n 2\cos(k\alpha_n)] \quad (12)$$

The desired modulating amplitude can be defined as a ratio of the peak output voltage to the input voltage, further simplifying the equation. With an equation for the odd harmonics, the harmonics past the fundamentals are then set to zero. A system of transcendental equations is then created by substituting in odd values of k.

$$m_a = \frac{4}{\pi}[1 - 2\cos(\alpha_1) + 2\cos(\alpha_2) - 2\cos(\alpha_3)], \quad (13)$$

$$0 = \frac{4}{3\pi}[1 - 2\cos(3\alpha_1) + 2\cos(3\alpha_2) - 2\cos(3\alpha_3)] \quad (14)$$

$$0 = \frac{4}{5\pi}[1 - 2\cos(5\alpha_1) + 2\cos(5\alpha_2) - 2\cos(5\alpha_3)] \quad (15)$$

where, m is the modulation index, $m = \frac{b_1}{V_{DC}}$.

The above transcendental equations can be solved to determine a sequence of switching angles to eliminate the low-order harmonics. The switching angles of the waveform will be adjusted to get the output voltage with a reduced total harmonic distortion (THD), mathematically given by:

$$THD = \frac{\sqrt{\sum_{k=3,5,7,\ldots}^{\infty}(b_k)^2}}{b_1} \quad (16)$$

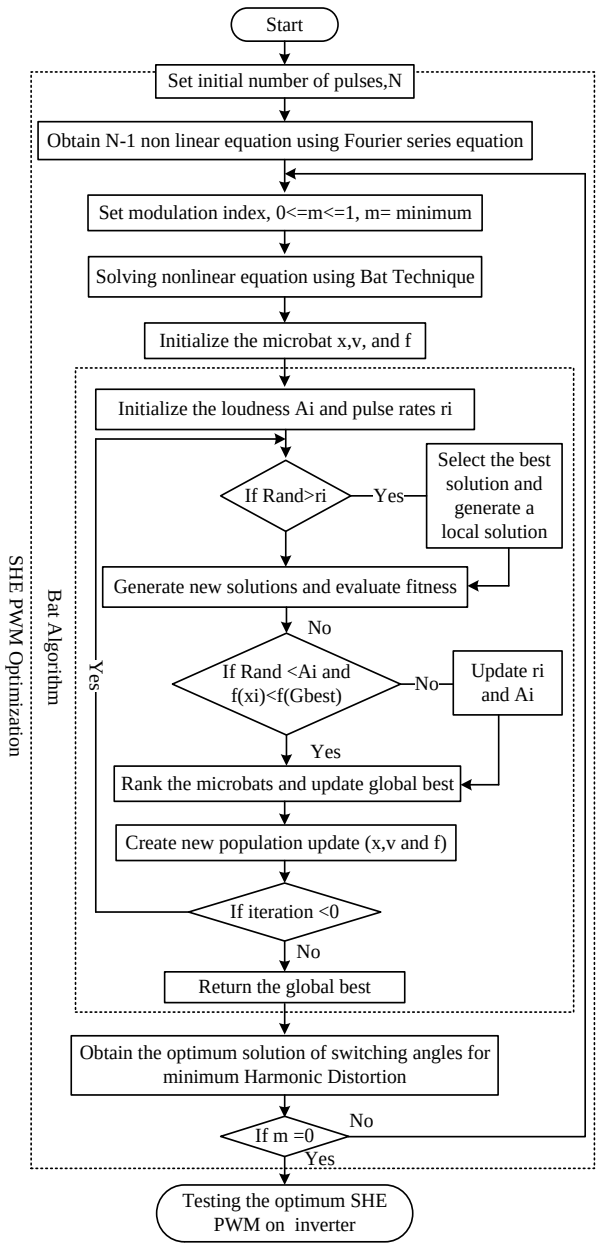

Fig. 5. Flow chart for the BAT Algorithm.

2168-6777 (c) 2021 IEEE. Personal use is permitted, but republication/redistribution requires IEEE permission. See http://www.ieee.org/publications_standards/publications/rights/index.html for more information.
Authorized licensed use limited to: Aalborg Universitetsbibliotek. Downloaded on June 03,2021 at 09:09:39 UTC from IEEE Xplore. Restrictions apply.

This article has been accepted for publication in a future issue of this journal, but has not been fully edited. Content may change prior to final publication. Citation information: DOI 10.1109/JESTPE.2021.3084737, IEEE Journal of Emerging and Selected Topics in Power Electronics

However, there is currently no closed-form solution for the system of equations. Therefore, the equations must be solved iteratively using a numerical method, especially when dealing with a large number of switching angles.

Hence, a Bat algorithm is adapted to calculate the switching angles for various amplitude modulation ratios. These values are interpolated depending on the actual value of the amplitude needed and eliminates the problem of flexibility associated with conventional and offline switching angle calculations.

B. Optimization of SHE-PWM

The Bat algorithm was initially introduced by Yang [33] and has been promising in terms of efficiency for global optimization. The echolocation parameters of the microbats and frequency interval constraints associated with them were adapted to develop the bat function, which is implemented using PSIM for optimization of PWM for transformerless inverters. A step-by-step procedure is depicted using the flow chart in Fig. 5. Further, the objective space curve identifies the best fitness obtained for total iterations performed. The best fitness point is observed before 20 iterations. The switching angles at the corresponding global best are achieved at a modulation index of 0.85.

Further, the BAT algorithm is executed for regulating the voltage output of the proposed inverter topology under varying load conditions. Initially, the voltage signals are sampled using the internal 10-bit analog-to-digital converter inside the field-programmable gate array (FPGA). The local minimum convergence is boosted by the algorithm, and for improving the algorithm performance, the finite state machine is implemented by manipulating the maximum of parallelism. Further, most of the literature presented aim at reducing the time of execution. The research presented in this paper focuses on the generation of dynamic bat algorithm using parallel processing [34]. The parallel processing helps in speeding up the processing of the algorithm by utilizing uniform distribution method for achieving an optimum solution with considerable processing time.

V. EXPERIMENT VERIFICATION

To verify the analysis of the operation of DG and the developed control technique in SA mode, simulation analysis has been carried out by using the system depicted in Fig. 3. A photovoltaic array is considered to operate as a DG under standard test conditions with varying loads.

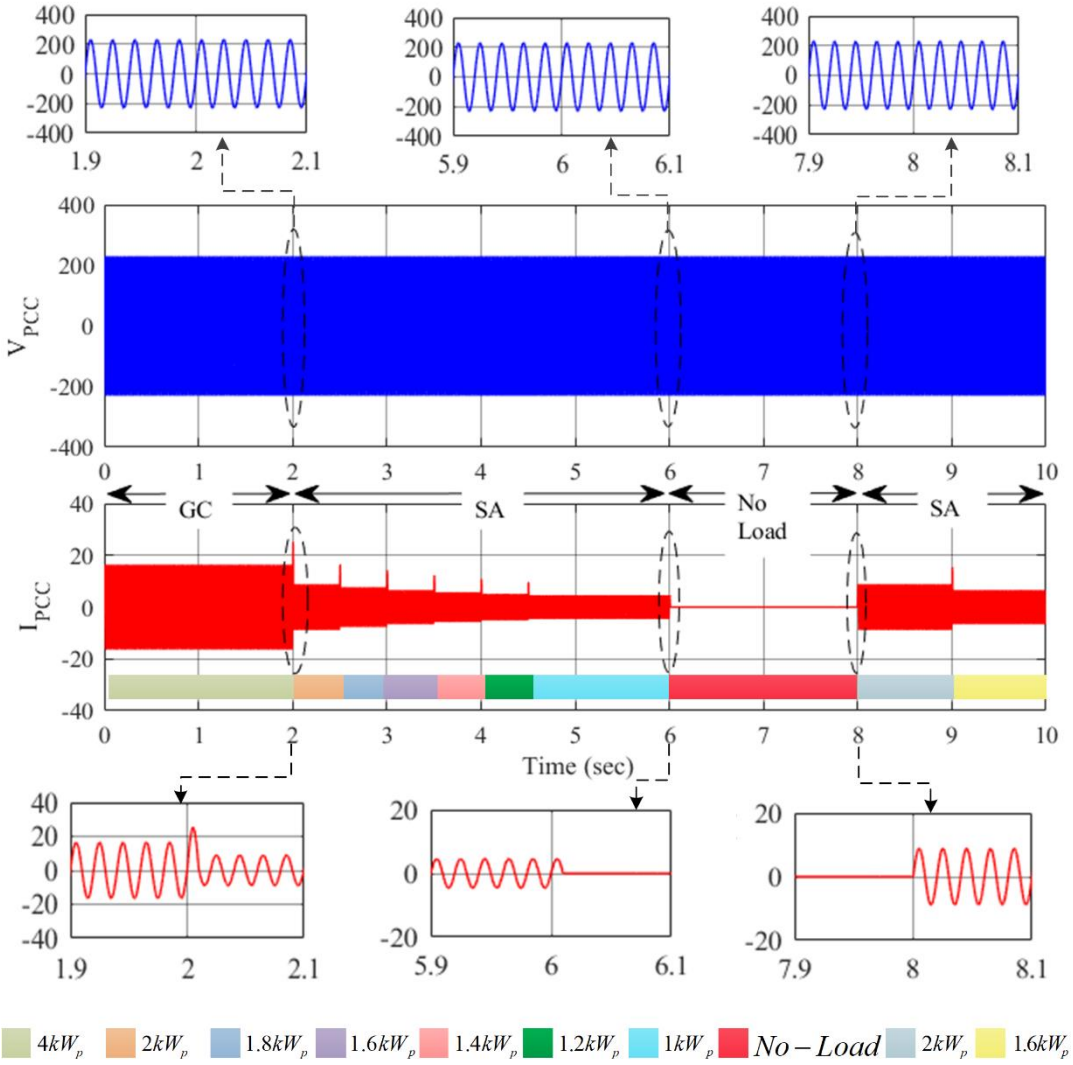

Fig. 6. Grid-connected to stand-alone mode operation along with load switching of resistive load

2168-6777 (c) 2021 IEEE. Personal use is permitted, but republication/redistribution requires IEEE permission. See http://www.ieee.org/publications_standards/publications/rights/index.html for more information.
Authorized licensed use limited to: Aalborg Universitetsbibliotek. Downloaded on June 03,2021 at 09:09:39 UTC from IEEE Xplore. Restrictions apply.

This article has been accepted for publication in a future issue of this journal, but has not been fully edited. Content may change prior to final publication. Citation information: DOI 10.1109/JESTPE.2021.3084737, IEEE Journal of Emerging and Selected Topics in Power Electronics

The parameters of the simulated system and its controller can be found in Table I. The voltage control loop along with the optimized SHE-PWM controller is connected in the feedback loop with the system to illustrate the controllability and conditioning of energy in SA operation.

TABLE. I
Design parameters for Stand-alone (SA) PV system

Parameter	Value
Photovoltaic generation	$2\ kWp$
Boost converter switching frequency (f_{sw})	$5\ kHz$
Boost converter inductance	$0.1\ mH$
DC link capacitance	$2000\ \mu F$
LCL filter converter side inductance	$0.48\ mH$
Inverter Switching Frequency	$10\ kHz$
Variation in converter current	10% of the maximum converter current
Load side inductance	$0.24\ mH$
Filter Capacitance [35]	$2.0101\ uF$
Damping Resistance	$0.5\ ohms$

1. *Simulation result*

The simulations are carried out with linear and nonlinear loads under resistive and inductive loading conditions. Due to controller implementation on the system, whenever there is a change in load, the output of the system is regulated within the limits specified as in [36]. The action of the developed controller from GC mode to stand alone mode under load shedding and varying load condition with resistive load is shown in Fig. 6. Initially, the simulated grid system with load shedding algorithm and the control algorithm are operating in a grid connected mode. Here, from 0 secs the expression for voltage amplitude is estimated by the load shedding algorithm through the per unit values, and the slope of the voltage amplitude is calculated as given in (3). Based on the estimated slope of the voltage amplitude, the current is measured as shown in (4). Further, at 2 secs, the distributed generation is intentionally disconnected from the grid. As the main power grid is out, the distributed generation unit continues to inject pre-determined optimum power and causes voltage and frequency transients depending on the degree of power difference. These transients can be observed at 2 secs i.e., the intentional disconnection instant. Further, the power difference creates a drift between the estimated voltage and nominal values of voltage and frequency, effecting the slope of the voltage amplitude. Here, based on the estimated current, the required load shedding is calculated from (5) to maintain a balance between the supply and demand. After $t = 2\ sec$, as the DG is disconnected from the grid and the full-bridge inverter operates with the developed controller at $2\ kWp$ load. The load is varied for identifying the capability of the controller in handling transients at the voltage and. At $t = 6\ sec$, the full-bridge inverter is operated at no load. At this instant, the load voltage is regulated without any transients. Further at $t = 8\ sec$, the DG is operated with $2\ kWp$ load. A transient current cycle is observed at this instant, where the operation changes from no load to loaded condition without any effect on the load voltage.

Further, the action of the developed controller on the SA operation for inductive (RL) load is observed and the results are shown in Fig. 7. Initially, the system is operated at $1.5\ kWp$ RL load, and at $t = 0.25\ sec$, the load is increased to $2\ kWp$. From the Fig. 7, it can be observed that at the instant of load variation, the load voltage is regulated without any transients.

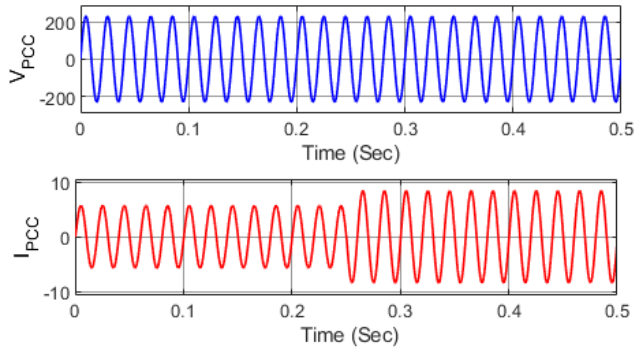

Fig. 7. Stand-alone operation of the full-bridge inverter with varying inductive load

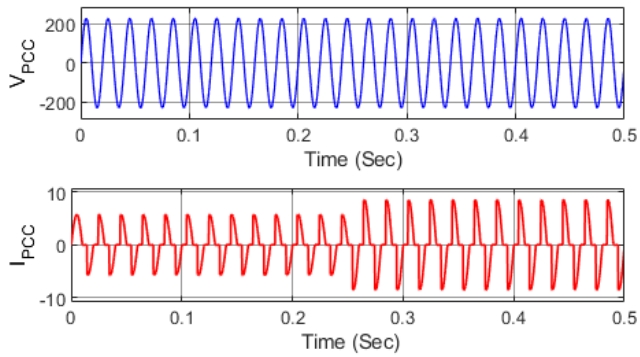

Fig. 8. Stand-alone operation of the full-bridge inverter with varying nonlinear resistive load

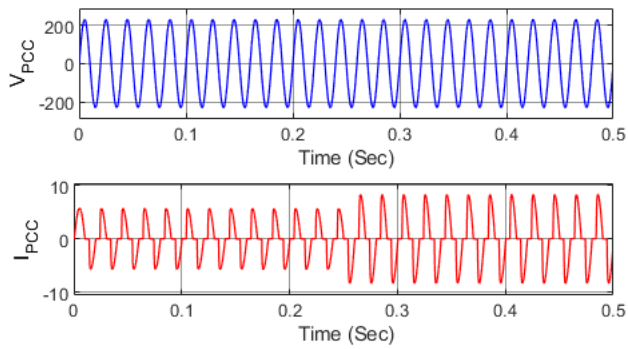

Fig. 9. Stand-alone operation of the full-bridge inverter with varying nonlinear inductive load

In addition to the linear resistive and inductive loads, the action of the developed controller is tested on the nonlinear loads. Initially, a nonlinear resistive load of $1.5\ kWp$ is operated in SA mode with the full-bridge inverter. At $0.25\ secs$, the load is increased to $2kWp$. The corresponding load voltage and load current are shown in Fig. 8. Further, a nonlinear inductive load of $1.5\ kWp$ is operated in SA mode with the full-bridge inverter. The step load change from $1.5\ kWp$ to $2kWp$ is identified at $0.25\ secs$ and the corresponding load voltage and load current are shown in Fig. 9.

2168-6777 (c) 2021 IEEE. Personal use is permitted, but republication/redistribution requires IEEE permission. See http://www.ieee.org/publications_standards/publications/rights/index.html for more information.
Authorized licensed use limited to: Aalborg Universitetsbibliotek. Downloaded on June 03,2021 at 09:09:39 UTC from IEEE Xplore. Restrictions apply.

This article has been accepted for publication in a future issue of this journal, but has not been fully edited. Content may change prior to final publication. Citation information: DOI 10.1109/JESTPE.2021.3084737, IEEE Journal of Emerging and Selected Topics in Power Electronics

1. *Test Results*

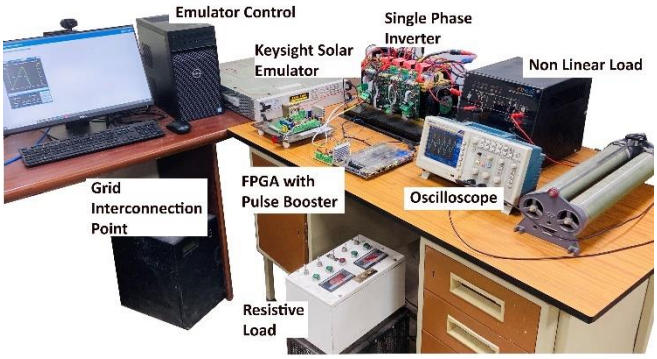

Fig. 10. Experimental Setup

The developed voltage control loop with optimized SHE-PWM is experimentally validated by digitally realizing the controller through Altera DE2-115 cyclone IV field-programmable gate array. The Quartus II programming platform [37] to generate the different gating signals suitable to drive the switches of the system. Further, the PV array with the rated power of $2\,kWp$ is realized using an Agilent Keysight PV simulator, which emulates the behavior of the PV arrays according to the PV cell parameters and the irradiance profile. The operation of GC mode is achieved with the help of a chroma grid simulator and the experimental setup of the GC PV system with a developed controller is illustrated in Fig. 10.

The operation of the DGs from GC mode to SA mode is identified by measuring the grid voltage, load voltage, and load current as shown in Fig. 11. Initially, the system is being operated in GC mode, and the output shows the grid voltage and load voltage with $1.2\,kWp$ load. After $30\,ms$, the PV system is disconnected from the grid to operate in SA mode and the grid voltage is observed to be zero. The operation of the inverter in SA mode with $1.2\,kWp$ load is shown in Fig. 12. The voltage THD of the inverter operating in SA mode with $1.2\,kWp$ load is observed to be 2.33 %, as shown in Fig. 13.

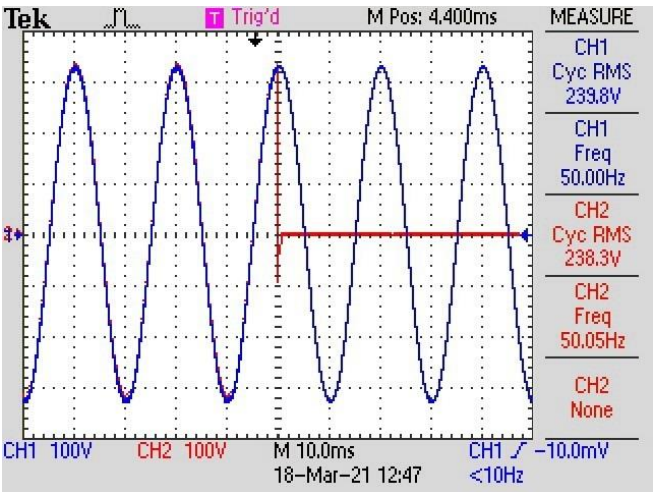

(a) Load voltage at Grid

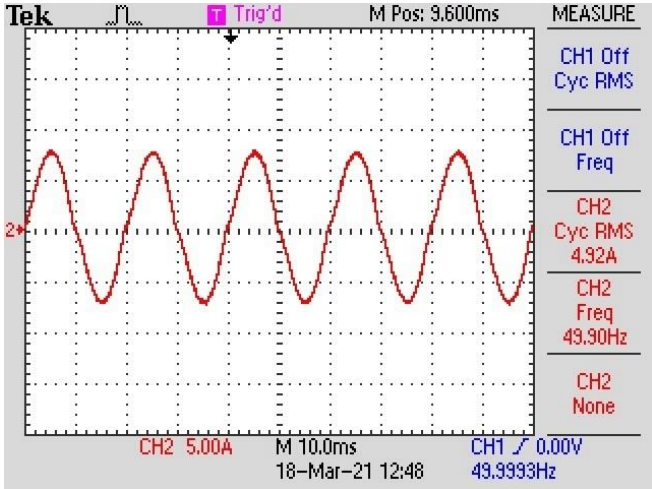

(b) Load current during transition between grid-connected to standalone mode

Fig. 11. Grid voltage, load voltage, and load current during grid-connected to stand-alone operation

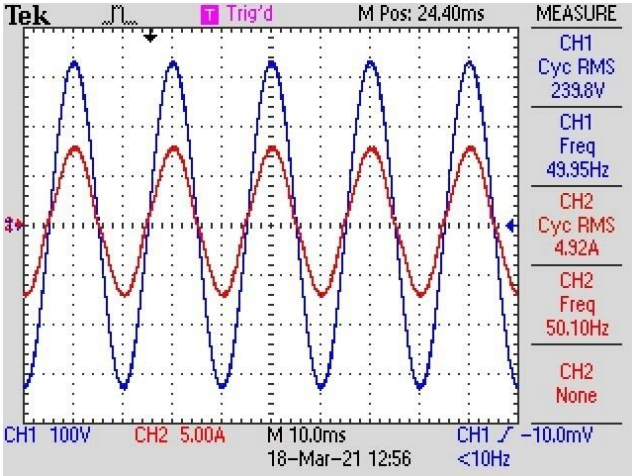

Fig. 12. Load voltage and load current during stand-alone operation

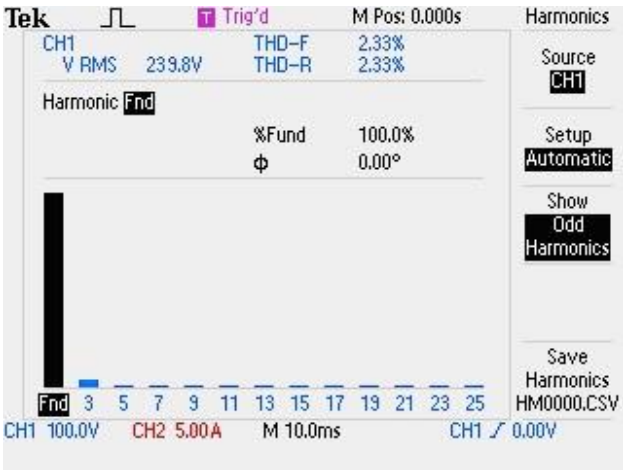

Fig. 13. Voltage THD for stand-alone operation of the inverter

The operation of the inverter from no-load condition to $1.2\,kWp$ is shown in Fig. 14. Initially, the inverter is operated under no-load condition, and at $t = 100\,ms$ the $1.2\,kWp$ load is switched into the system.

2168-6777 (c) 2021 IEEE. Personal use is permitted, but republication/redistribution requires IEEE permission. See http://www.ieee.org/publications_standards/publications/rights/index.html for more information.
Authorized licensed use limited to: Aalborg Universitetsbibliotek. Downloaded on June 03,2021 at 09:09:39 UTC from IEEE Xplore. Restrictions apply.

This article has been accepted for publication in a future issue of this journal, but has not been fully edited. Content may change prior to final publication. Citation information: DOI 10.1109/JESTPE.2021.3084737, IEEE Journal of Emerging and Selected Topics in Power Electronics

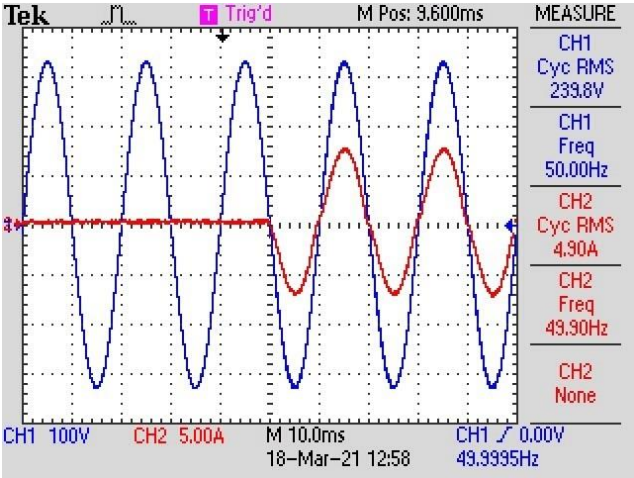

Fig. 14. Load voltage and load current during varying load in stand-alone operation

The voltage THD of the inverter operating from no load to peak load in SA mode is observed to be 2.51 %, as shown in Fig. 15.

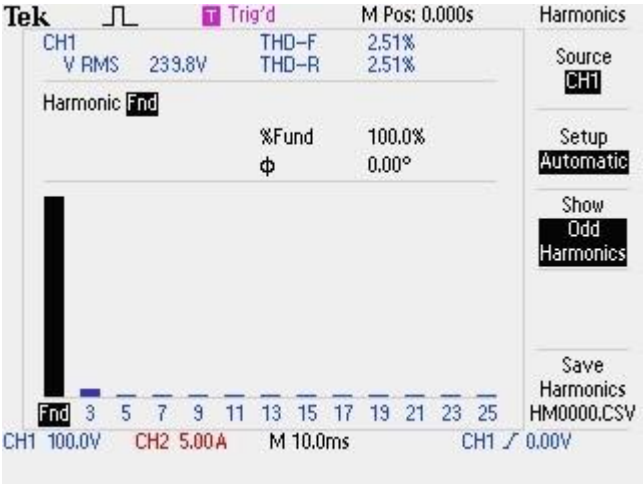

Fig. 15. Voltage THD for stand-alone operation of inverter during varying load

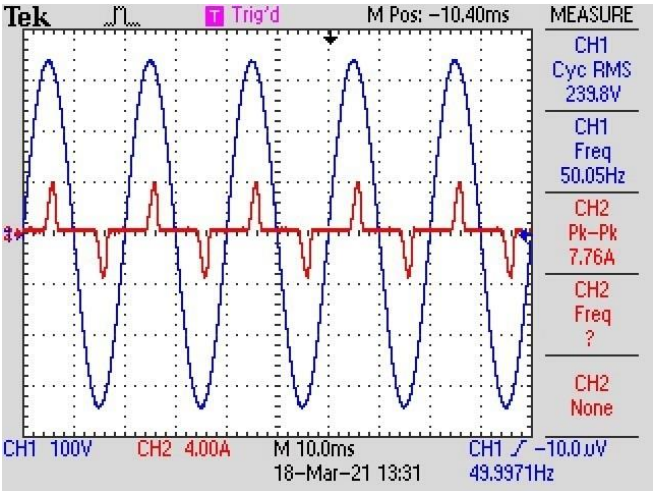

Fig. 16. Steady-state response of inverter under stand-alone operation with 0.88 KWp nonlinear load.

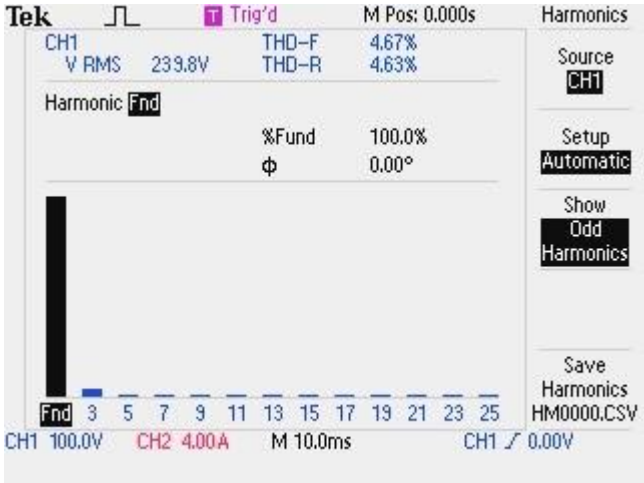

Fig. 17. THD of inverter voltage output operating under 0.88 kWp nonlinear load

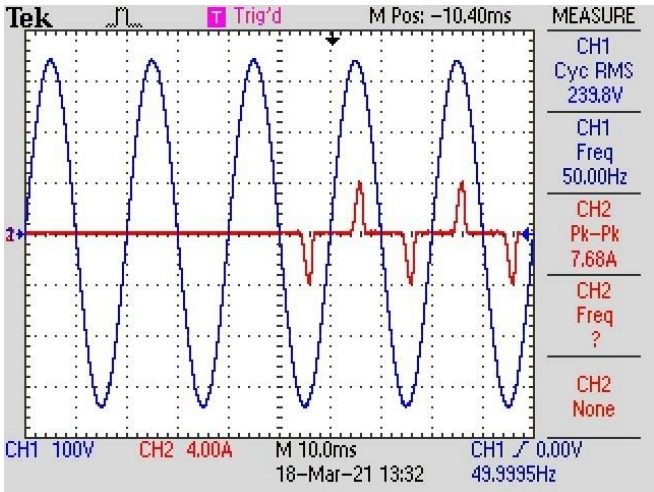

Fig. 18. Load voltage and load current during varying non-linear load in stand-alone operation

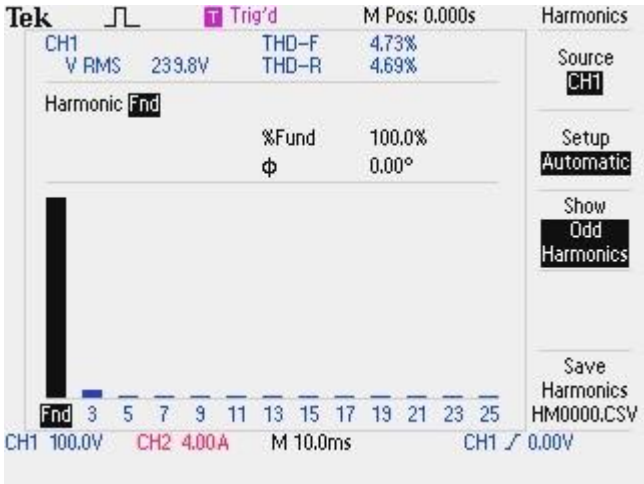

Fig. 19. Voltage THD for stand-alone operation of inverter during varying non-linear load

Further, the inverter is operated with a rectifier controlled resistive load to depict the operation of the digitally realized controller on the nonlinear load. The load voltage and load current during the operation of the PV system for a 0.88 kWp load is shown in Fig. 16. Besides, the FFT analysis for the voltage of the inverter operating with nonlinear load is

2168-6777 (c) 2021 IEEE. Personal use is permitted, but republication/redistribution requires IEEE permission. See http://www.ieee.org/publications_standards/publications/rights/index.html for more information.
Authorized licensed use limited to: Aalborg Universitetsbibliotek. Downloaded on June 03,2021 at 09:09:39 UTC from IEEE Xplore. Restrictions apply.

This article has been accepted for publication in a future issue of this journal, but has not been fully edited. Content may change prior to final publication. Citation information: DOI 10.1109/JESTPE.2021.3084737, IEEE Journal of Emerging and Selected Topics in Power Electronics

observed to be 4.67 %, as shown in Fig. 17. Similarly, the operation of the system with modified SHE-PWM under varying non-linear load is shown in Fig. 18, and the corresponding voltage THD is identified to be 4.73% as shown in Fig. 19.

It is noted that the developed strategy with a modified modulation method succeeded in achieving THD complying with the IEEE 1547 Standard (THD 5 %). Further, the THD obtained by the action of modified SHE PWM controller is compared with the conventional SHE PWM and widely used PI controllers, and the corresponding observations are tabulated in Table II.

TABLE. II
Comparison between actions of various controllers for THD minimization

Parameter	Modified SHE-PWM with LCL filter	SHE-PWM with LCL filter	PI controller with SPWM for LCL filter
Nominal Voltage	240 V	240 V	240 V
Total Load (Non-Varying)	1.2 kWp linear load	1.2 kWp linear load	1.2 kWp linear load
	1.15 kWp nonlinear load	1.15 kWp nonlinear load	1.15 kWp nonlinear load
Switching Frequency	10 kHz	10 kHz	10 kHz
Modulation Index	Variable (Continuously updated based on transients in output voltage)	0.85	0.85
LCL Filter	L_1: 0.48 mH L_2: 0.24 mH C: 2 uF	L_1: 2.5 mH L_2: 1.25 mH C: 3 uF	L_1: 2.5 mH L_2: 1.25 mH C: 3 uF
THD under linear load	2.33 %	5 %	5.7 %
THD under nonlinear load	4.67 %	7.8 %	11.6 %

Further, the parallel processing approach used to generate the dynamic bat algorithm aims at speeding up the process by using a uniform distribution method. This achieved optimum solution with a significant execution time. Generally, the execution time depends on the number of iterations allocated to achieve the optimal solution, and for the bat algorithm, it takes (1590) clock cycles for the processing time of one iteration. Hence, as the maximum number of iterations observed to operate the SHE PWM are 20, the total execution time is 31.8 ms.

VI. CONCLUSION

This paper presented the development of a control strategy for operating DGs in both SA and GC modes. The SA control featured a voltage control loop capable of overcoming the drawbacks due to load shedding or load switching, whereas the control GC system is achieved by performing current control operation. Further, the harmonics in the system especially during the transition and load shedding or load switching are eliminated by adopting a SHE-PWM scheme. The performance of the harmonic elimination scheme is enhanced by optimizing it with a Bat algorithm which eliminates the problem of flexibility associated with conventional and offline switching angle calculations in the PWM technique. The developed system is verified for various performance characteristics such as reduced THD and improved efficiency by simulations and experiments on a 2 kWp photovoltaic system. The results depicted that the output voltage is regulated for varying load conditions, and the THD is observed to be 2.4 % under varying load conditions.

REFERENCES

[1] J. C. J. C. Vasquez *et al.*, "Adaptive Droop Control Applied to Voltage-Source Inverters Operating in Grid-Connected and Islanded Modes," *IEEE Trans. Ind. Electron.*, vol. 56, no. 10, pp. 4088–4096, Oct. 2009.

[2] J. Selvaraj and N. A. N. A. Rahim, "Multilevel Inverter For Grid-Connected PV System Employing Digital PI Controller," *IEEE Trans. Ind. Electron.*, vol. 56, no. 1, pp. 149–158, Jan. 2009.

[3] G. Franceschini, E. Lorenzani, C. Tassoni, and A. Bellini, "Synchronous Reference Frame Grid Current Control for Single-Phase Photovoltaic Converters," in *2008 IEEE Industry Applications Society Annual Meeting*, 2008, pp. 1–7.

[4] M. E. Haque, M. Negnevitsky, and K. M. Muttaqi, "A Novel Control Strategy for a Variable-Speed Wind Turbine With a Permanent-Magnet Synchronous Generator," *IEEE Trans. Ind. Appl.*, vol. 46, no. 1, pp. 331–339, 2010.

[5] T. C. Green and M. Prodanović, "Control of inverter-based micro-grids," *Electr. Power Syst. Res.*, vol. 77, no. 9, pp. 1204–1213, Jul. 2007.

[6] O. J. K. Oghorada, L. Zhang, B. A. Esan, and E. Dickson, "Carrier-based sinusoidal pulse-width modulation techniques for flying capacitor modular multi-level cascaded converter," *Heliyon*, vol. 5, no. 12, pp. 1–16, Dec. 2019.

[7] R. Wang, W. Wang, R. Liu, J. Zhang, and X. Mu, "Carrier-based pulse-width modulation control strategy of five-phase six-bridge indirect matrix converter under unbalanced load," *IET Power Electron.*, vol. 10, no. 14, pp. 1932–1942, Nov. 2017.

[8] J. F. Khan, S. M. A. Bhuiyan, K. M. Rahman, and G. V. Murphy, "Space vector PWM for a two-phase VSI," *Int. J. Electr. Power Energy Syst.*, vol. 51, pp. 265–277, Oct. 2013.

[9] J. N. da Silva, A. J. S. Filho, D. A. Fernandes, A. P. N. Tahim, E. R. C. da Silva, and F. F. Costa, "A discrete repetitive current controller for single-phase grid-connected inverters," in *2017 Brazilian Power Electronics Conference (COBEP)*, 2017, pp. 1–6.

[10] M. A. Khan, A. Haque, and V. S. B. Kurukuru, "Performance assessment of stand-alone transformerless inverters," *Int. Trans. Electr. Energy Syst.*, vol. 30, no. 1, pp. 1–20, Jan. 2020.

[11] M. A. Khan, A. Haque, and V. S. B. Kurukuru, "Intelligent control of a novel transformerless inverter topology for photovoltaic applications," *Electr. Eng.*, vol. 102, no. 2, pp. 627–641, Jun. 2020.

[12] Y. Han, A.-T. T. Jiang, E. A. A. A. A. Coelho, and J. M. Guerrero, "Optimal Performance Design Guideline of Hybrid Reference Frame Based Dual-Loop Control Strategy for Stand-Alone Single-Phase Inverters," *IEEE Trans. Energy Convers.*, vol. 33, no. 2, pp. 730–740, Jun. 2018.

[13] N. Kumar, T. K. Saha, and J. Dey, "Sliding mode control, implementation and performance analysis of standalone PV fed dual inverter," *Sol. Energy*, vol. 155, pp. 1178–1187, 2017.

[14] B. Talbi, F. Krim, A. Laib, and A. Sahli, "Model predictive voltage control of a single-phase inverter with output LC filter for stand-alone renewable energy systems," *Electr. Eng.*, vol. 102, no. 3, pp. 1073–1082, Sep. 2020.

[15] P. Cortes, G. Ortiz, J. I. Yuz, J. Rodriguez, S. Vazquez, and L. G. Franquelo, "Model Predictive Control of an Inverter With Output LC Filter for UPS Applications," *IEEE Trans. Ind. Electron.*, vol. 56, no. 6, pp. 1875–1883, Jun. 2009.

[16] H. S. Patel and R. G. Hoft, "Generalized Techniques of Harmonic Elimination and Voltage Control in Thyristor Inverters: Part I-Harmonic Elimination," *IEEE Trans. Ind. Appl.*, vol. IA-9, no. 3, pp. 310–317, 1973.

[17] H. S. PATEL and R. G. HOFT, "Generaiized Techniques of Harmonic Elimination and Voltage Control in Ihyristor Inverters: Part II-Voltage Control Techniques," *IEEE Trans. Ind. Appl.*, vol. 1A, no. 5, pp. 666–673, 1974.

[18] S. Ahmad, Z. A. Ganie, I. Ashraf, and A. Iqbal, "Harmonics Minimization in 3-Level Inverter Waveform and its FPGA Realization," in *2018 3rd International Innovative Applications of Computational Intelligence on Power, Energy and Controls with their Impact on Humanity (CIPECH)*, 2018, pp. 1–5.

[19] S. Ahmad, M. Meraj, A. Iqbal, and I. Ashraf, "Selective harmonics

2168-6777 (c) 2021 IEEE. Personal use is permitted, but republication/redistribution requires IEEE permission. See http://www.ieee.org/publications_standards/publications/rights/index.html for more information.
Authorized licensed use limited to: Aalborg Universitetsbibliotek. Downloaded on June 03,2021 at 09:09:39 UTC from IEEE Xplore. Restrictions apply.

This article has been accepted for publication in a future issue of this journal, but has not been fully edited. Content may change prior to final publication. Citation information: DOI 10.1109/JESTPE.2021.3084737, IEEE Journal of Emerging and Selected Topics in Power Electronics

elimination in multilevel inverter by a derivative-free iterative method under varying voltage condition," *ISA Trans.*, vol. 92, pp. 241–256, Sep. 2019.

[20] S. Ahmad, M. Al-Hitmi, A. Iqal, I. Ashraf, M. Meraj, and S. Padmanaban, "Low-order harmonics control in staircase waveform useful in high-power application by a novel technique," *Int. Trans. Electr. Energy Syst.*, vol. 29, no. 3, p. e2769, Mar. 2019.

[21] S. Ahmad and A. Iqbal, "Switching Angles Computations Using PSO in Selective Harmonics Minimization PWM," 2021, pp. 437–461.

[22] K. Ganesan, K. Barathi, P. Chandrasekar, and D. Balaji, "Selective Harmonic Elimination of Cascaded Multilevel Inverter Using BAT Algorithm," *Procedia Technol.*, vol. 21, pp. 651–657, 2015.

[23] M. Yingram and S. Premrudeepreechacharn, "Over/Undervoltage and Undervoltage Shift of Hybrid Islanding Detection Method of Distributed Generation," *Sci. World J.*, vol. 2015, pp. 1–11, 2015.

[24] Q. Sun, J. M. Guerrero, T. Jing, R. Quintero, Juan Carlos Vasquez Yang, J. C. Vasquez, and R. Yang, "An Islanding Detection Method by Using Frequency Positive Feedback Based on FLL for Single-Phase Microgrid," *IEEE Trans. Smart Grid*, vol. 8, no. 4, pp. 1–10, Jul. 2016.

[25] X. Liao, Z. Guo, D. Sha, and X. Liao, "Voltage magnitude and frequency control of three-phase voltage source inverter for seamless transfer," *IET Power Electron.*, vol. 7, no. 1, pp. 200–208, Jan. 2014.

[26] D. N. Gaonkar, G. N. Pillai, and R. N. Patel, "Seamless Transfer of Microturbine Generation System Operation Between Grid-connected and Islanding Modes," *Electr. Power Components Syst.*, vol. 37, no. 2, pp. 174–188, Jan. 2009.

[27] R. Majumder, A. Ghosh, G. Ledwich, and F. Zare, "Control of parallel converters for load sharing with seamless transfer between grid connected and islanded modes," in *2008 IEEE Power and Energy Society General Meeting - Conversion and Delivery of Electrical Energy in the 21st Century*, 2008, pp. 1–7.

[28] S. Hirodontis and H. Li, "An adaptive load shedding method for intentional islanding," in *2009 International Conference on Clean Electrical Power*, 2009, pp. 300–303.

[29] R. G. Wandhare, S. Thale, and V. Agarwal, "Design of a photovoltaic power conditioning system for hierarchical control of a microgrid," in *2014 IEEE 40th Photovoltaic Specialist Conference (PVSC)*, 2014, pp. 3144–3149.

[30] M. Marzband, M. M. Moghaddam, M. F. Akorede, and G. Khomeyrani, "Adaptive load shedding scheme for frequency stability enhancement in microgrids," *Electr. Power Syst. Res.*, vol. 140, pp. 78–86, Nov. 2016.

[31] J. M. Espi Huerta, J. Castello-Moreno, J. R. Fischer, and R. Garcia-Gil, "A Synchronous Reference Frame Robust Predictive Current Control for Three-Phase Grid-Connected Inverters," *IEEE Trans. Ind. Electron.*, vol. 57, no. 3, pp. 954–962, Mar. 2010.

[32] M. A. Memon, S. Mekhilef, M. Mubin, and M. Aamir, "Selective harmonic elimination in inverters using bio-inspired intelligent algorithms for renewable energy conversion applications: A review," *Renew. Sustain. Energy Rev.*, vol. 82, pp. 2235–2253, Feb. 2018.

[33] X. S. Yang, "A new metaheuristic Bat-inspired Algorithm," *Stud. Comput. Intell.*, vol. 284, pp. 65–74, 2010.

[34] J. Kan, Y. Wu, Y. Tang, S. Member, S. Xie, and L. Jiang, "Hybrid Control Scheme for Photovoltaic Micro-Inverter with Adaptive Inductor," *IEEE Trans. Power Electron.*, vol. PP, no. c, p. 1, 2018.

[35] C.-L. Chen, J.-S. Lai, Y.-B. Wang, S.-Y. Park, and H. Miwa, "Design and Control for LCL-Based Inverters with Both Grid-Tie and Standalone Parallel Operations," in *2008 IEEE Industry Applications Society Annual Meeting*, 2008, pp. 1–7.

[36] Goverment of India, "National electrical code," 2011.

[37] J. S. Parab, R. S. Gad, and G. M. Naik, "Getting Hands on Altera® Quartus® II Software," in *Hands-on Experience with Altera FPGA Development Boards*, New Delhi: Springer India, 2018, pp. 19–37.

Mohammed Ali Khan (S'17) received his B.Tech. degree in Electrical and Electronics Engineering from Karunya University, Coimbatore, India, in 2013, M.Tech. degree in Power System from Amity University, Noida, India, in 2016 and Ph.D. degree from the Department of Electrical Engineering, Jamia Millia Islamia (A Central University), New Delhi, India, in 2021.

He was a Visiting Researcher at the Center of Reliable Power Electronics, Aalborg University, Aalborg, Denmark, from October to December 2020. He had also worked as Guest Faculty in the Department of Electrical Engineering, Jamia Millia Islamia (A Central University), New Delhi, India from 2017 to 2020. He has many publications in peer-reviewed journals and presented his research articles in several international conferences. His area of research is artificial intelligence, power electronics, and their application in renewable energy systems, power quality improvements, and reliability.

Ahteshamul Haque (M'13-SM'14) received the B.Tech. degree in Electrical Engineering from Aligarh Muslim University, Aligarh, India, in 1999, the master's degree in Electrical Engineering from IIT Delhi, New Delhi, India, in 2000, and the Ph.D. degree in Electrical Engineering from the Department of Electrical Engineering, Jamia Millia Islamia University, New Delhi, India, in 2015. Prior to academics, he was working in the research and development unit of world reputed multinational industries and his work is patented in the USA and Europe. He is currently a Professor (Assistant-Senior Scale) with the Department of Electrical Engineering, Jamia Millia Islamia University. He has established Advance Power Electronics Research Laboratory, Department of Electrical Engineering, Jamia Millia Islamia. He is working as a Principal Investigator of the MHRD-SPARC project and other research and development projects. He is the recipient of IEEE PES Outstanding Engineer Award for the year 2019. He has authored or co-authored around 100 publications in international journals and conference proceedings. He is senior Member of IEEE. His current research interests include power converter topologies, control of power converters, renewable energy, and energy efficiency, reliability analysis, electric vehicle operations.

V. S. Bharath Kurukuru (S'18) received his B.Tech. degree in Electrical and Electronics Engineering from Avanthi's Research and Technological Academy, Vizianagaram, India, in 2014, and M.Tech. degree in Power Systems from Amity University, Noida, India, in 2016. He is currently pursuing his Ph.D. degree in the Advanced Power Electronics Research Laboratory, Department of Electrical Engineering, Jamia Millia Islamia (A Central University), New Delhi, India.

He was a Visiting Researcher at the Center of Reliable Power Electronics, Aalborg University, Aalborg, Denmark, from August to October 2019. His area of research is fault diagnosis, condition monitoring, and reliability of power electronics converters in renewable energy systems and electric vehicles.

Huai Wang (M'12-SM'17) received a BE degree in electrical engineering from Huazhong University of Science and Technology, Wuhan, China in 2007 and a PhD degree in power electronics from the City University of Hong Kong in 2012. He is currently Professor with Department of Energy Technology at Aalborg University, Denmark, where he leads the group of Reliability of Power Electronic Converters. He was a Visiting Scientist with the ETH Zurich, Switzerland, from Aug. to Sep. 2014, and with the Massachusetts Institute of Technology (MIT), USA, from Sep. to Nov. 2013. He was with the ABB Corporate Research Center, Switzerland in 2009. His research addresses the fundamental challenges in modelling and validation of power electronic component failure mechanisms and application issues in system-level predictability, condition monitoring, circuit architecture, and robustness design.

Dr. Wang received the Richard M. Bass Outstanding Young Power Electronics Engineer Award from the IEEE Power Electronics Society in 2016, and the Green Talents Award from the German Federal Ministry of Education and Research in 2014. He is currently the Chair of IEEE PELS/IAS/IES Chapter in Denmark. He serves as an Associate Editor of IET Electronics Letters, IEEE JOURNAL OF EMERGING AND SELECTED TOPICS IN POWER ELECTRONICS, and IEEE TRANSACTIONS ON POWER ELECTRONICS.

2168-6777 (c) 2021 IEEE. Personal use is permitted, but republication/redistribution requires IEEE permission. See http://www.ieee.org/publications_standards/publications/rights/index.html for more information.
Authorized licensed use limited to: Aalborg Universitetsbibliotek. Downloaded on June 03,2021 at 09:09:39 UTC from IEEE Xplore. Restrictions apply.

Frede Blaabjerg (S'86–M'88–SM'97–F'03) was with ABB-Scandia, Randers, Denmark, from 1987 to 1988. From 1988 to 1992, he got the PhD degree in Electrical Engineering at Aalborg University in 1995. He became an Assistant Professor in 1992, an Associate Professor in 1996, and a Full Professor of power electronics and drives in 1998. From 2017 he became a Villum Investigator. He is honoris causa at University Politehnica Timisoara (UPT), Romania and Tallinn Technical University (TTU) in Estonia.

His current research interests include power electronics and its applications such as in wind turbines, PV systems, reliability, harmonics and adjustable speed drives. He has published more than 600 journal papers in the fields of power electronics and its applications. He is the co-author of four monographs and editor of ten books in power electronics and its applications. He has received 33 IEEE Prize Paper Awards, the IEEE PELS Distinguished Service Award in 2009, the EPE-PEMC Council Award in 2010, the IEEE William E. Newell Power Electronics Award 2014, the Villum Kann Rasmussen Research Award 2014, the Global Energy Prize in 2019 and the 2020 IEEE Edison Medal. He was the Editor-in-Chief of the IEEE TRANSACTIONS ON POWER ELECTRONICS from 2006 to 2012. He has been Distinguished Lecturer for the IEEE Power Electronics Society from 2005 to 2007 and for the IEEE Industry Applications Society from 2010 to 2011 as well as 2017 to 2018. In 2019-2020 he served as a President of IEEE Power Electronics Society. He has been Vice-President of the Danish Academy of Technical Sciences.

He is nominated in 2014-2020 by Thomson Reuters to be between the most 250 cited researchers in Engineering in the world.

2168-6777 (c) 2021 IEEE. Personal use is permitted, but republication/redistribution requires IEEE permission. See http://www.ieee.org/publications_standards/publications/rights/index.html for more information.
Authorized licensed use limited to: Aalborg Universitetsbibliotek. Downloaded on June 03,2021 at 09:09:39 UTC from IEEE Xplore. Restrictions apply.